Hindawi
Mathematical Problems in Engineering
Volume 2021, Article ID 9505845, 18 pages
https://doi.org/10.1155/2021/9505845

Research Article

PWM-VSI Diagnostic and Reconfiguration Method Based on Fuzzy Logic Approach for SSTPI-Fed IM Drives under IGBT OCFs

Mohamed Ali Zdiri, Mohsen Ben Ammar, Fatma Ben Salem, and Hsan Hadj Abdallah

CEM Laboratory, National Engineering School of Sfax, Sfax, Tunisia

Correspondence should be addressed to Mohamed Ali Zdiri; mohamed-ali.zdiri@enis.tn

Received 2 May 2021; Revised 5 July 2021; Accepted 22 July 2021; Published 31 July 2021

Academic Editor: G. Muhiuddin

Due to the importance of the drive system reliability, several diagnostic methods have been investigated for the SSTPI-IM association in the literature. Based on the normalized currents and the current vector slope, this paper investigates a fuzzy diagnostic method for this association. The fuzzy logic technique is appealed in order to process the diagnosis variable symptoms and the faulty IGBT information. Indeed, the design, inputs, and rules of the fuzzy logic are distinct compared with the other existing diagnostic methods. The proposed fuzzy diagnostic method allows the best efficient detection and identification of the single and phase OCF of the SSTPI-IM association. Accordingly, after the fault detection and identification using this proposed FLC diagnostic method, a reconfiguration step of IGBT OCFs must be applied in order to compensate for these faults and ensure the drive system continuity. This reconfiguration is based on the change of the SSTPI-IM topology to the FSTPI-IM topology by activating or deactivating the used relays. Several simulation results utilizing a direct RFOC controlled SSTPI-IM drive system are investigated, showing the fuzzy diagnostic and reconfiguration methods' performances, their robustness, and their fast fault detection during distinct operating conditions.

1. Introduction

Given the reliability and efficiency, the SSTPI-IM association has been used in several industrial applications such as medical and military applications, renewable energy sources, robotics, and electric vehicles [1–3]. Due to the complexity of these systems, many faults can facilely occur. The occurrence of these faults can shut down the whole system, which can cause loss of continuity and energy. Consequently, special attention must be taken into account in the development of diagnostic methods for these defects.

In this paper, we focus only on the fault appearance in the switches of the SSTPI. Generally, the switch faults can be classified into three faults, which are OCF, intermittent fault, and SCF. In the SCF case, the IM cannot be more functional, and necessary system maintenance must be done. In this failure situation, a hardware safety circuit is presented in [4]. However, in the OCF case, a diagnosis method should be utilized in order to protect the drive system against secondary failures. It should be noted that the OCF, which is the subject of this paper, cannot shut down the drive system directly.

In 1976, the analytical redundancy method based on fault diagnosis and detection model is presented in [5]. Taking into consideration the technological evolution, several researchers began to develop new diagnostic methods for the SSTPI-IM association. A diagnostic method based on the analysis of the instantaneous frequency and current vector trajectory applied in a PWM-VSI in order to detect and isolate the switch fault is presented in [6]. Furthermore, based on the later proposed diagnostic method, an improved method, which can detect and identify multiple OCFs in a PWM-VSI, is presented in [7].

Several methods have been investigated based on Park's vector approach and the average current [8–12]. In [13], a new fault detection based on the DWT-NN technique is presented. Besides, a robust real-time diagnostic method for single and simultaneous OCF in sensorless vector-controlled

IM drives is presented in [14]. The authors in [15] have proposed a robust OCF diagnostic method in VSI-PMSM drives, which can detect and identify multiple IGBT OCFs. Furthermore, a diagnostic method based on an SMO and a half-bridge switching model is presented and applied in MMC [16]. In [17], in order to detect and identify the OCF, an FFT diagnostic method is used. Moreover, a real-time instant voltage error diagnostic method is presented in [18]. In order to detect, identify, and compensate the OCF, the authors in [19] have presented a fault-tolerant control and diagnosis method in MMC.

Among the presented diagnostic methods, one can highlight that some diagnostic methods can detect and identify a single OCF, and some diagnostic methods can detect and identify multiple OCFs. Expecting the single and multiple OCFs, there is a possibility of false alarms using the existed diagnostic methods during speed and load variations. Considering the above diagnostic methods, these false alarms can shut down all drive systems and cause power losses. In conclusion, in order to detect and identify precisely these faults without false alarms, the FLC theory is applied to precisely fuzzify the diagnosis of variable symptoms. FLC theory is utilized in a variety of applications, including drive systems, robotics, photovoltaic and wind energy, hybrid vehicles, and medical applications. In order to avoid the disadvantage of T-S (Takagi Sugeno) state estimation and to stabilize the nonlinear system, a combination of LMI (linear matrix inequality) and fuzzy model is presented in [20]. Moreover, the topic of T-S FTS (finite-time synchronization) for fuzzy complex dynamical networks with coupling delays through sampled-data control is discussed and presented in [21, 22]. Taking into account the organization evaluation efficiency and performance, a ranking framework based on FLC is presented in [23]. Also, the ranking of educational institutions based on fuzzy logic rule base is discussed and presented in [24].

An FLC diagnostic method that differs from other existing fault diagnostic strategies is suggested in order to enhance the fault detection and identification of IGBT OCFs against false alarms during speed and load variations. Based on the proposed FLC diagnostic method, single OCF and phase OCF can be detected and identified. This novel diagnostic method is based on the measured motor currents. The diagnosis variables are processed with FLC theory and the faulty switch information can be determined. It should be noted that, as compared to previous approaches, the suggested FLC diagnostic method simplifies the fault reconfiguration step. Indeed, in order to compensate for the switch OCF, a step of SSTPI-IM reconfiguration must be found. This reconfiguration strategy is based on the change of the SSTPI-IM topology to the FSTPI-IM topology by using a relay without redundant leg [25–27]. By using this novel FLC diagnostic method and reconfiguration strategy, the simulation results prove to confirm their high efficiency and performance in terms of detection and identification of the single OCF and phase OCF without power losses and false alarms during speed and load variations.

2. IGBT OCF Detection and Identification by Using Measured Currents

The given system in this work is made up of the following components as presented in Figure 1: grid, rectifier made up of six diodes, continuous bus, inverter, and IM. It should be noted that the SSTPI switches are controlled using a direct RFOC technique.

The proposed diagnostic method is based on the normalized currents and the current slope as presented in Figure 2. This method avoids the use of another extra hardware or sensors, which implies the low cost of its implementation.

It is well known that this method is found on Clarke's transformation as presented by

$$I_\alpha = \sqrt{\frac{3}{2}} I_{as}, \tag{1}$$

$$I_\beta = \frac{1}{\sqrt{2}} I_{as} + \sqrt{2}\, I_{bs}, \tag{2}$$

where I_{as}, I_{bs}, and I_{cs} are the measured stator currents.

According to Clarke's transformation, the vector modulus is given by

$$|\bar{I}|_s = \sqrt{I_\alpha^2 + I_\beta^2}. \tag{3}$$

In order to be robust versus the variations of the operating conditions, the normalized currents are presented by the following equation:

$$I_{nN} = \frac{I_n}{|\bar{I}_s|}, \tag{4}$$

where n represents the three phases (as, bs, and cs) and I_n denotes the balanced sinusoidal stator current as presented by

$$I_n = \begin{cases} I_{as} = I_{\max} \sin(w_s t) \\ I_{bs} = I_{\max} \sin\left(w_s t - \dfrac{2\pi}{3}\right), \\ I_{cs} = I_{\max} \sin\left(w_s t + \dfrac{2\pi}{3}\right) \end{cases} \tag{5}$$

where $I_{\max}$ represents the maximum amplitude and w_s represents the stator pulsation.

The vector modulus based on equations (3) and (5) is expressed by

$$|\bar{I}_s| = \sqrt{\frac{3}{2}} I_{\max}. \tag{6}$$

Accordingly, the normalized currents are given by

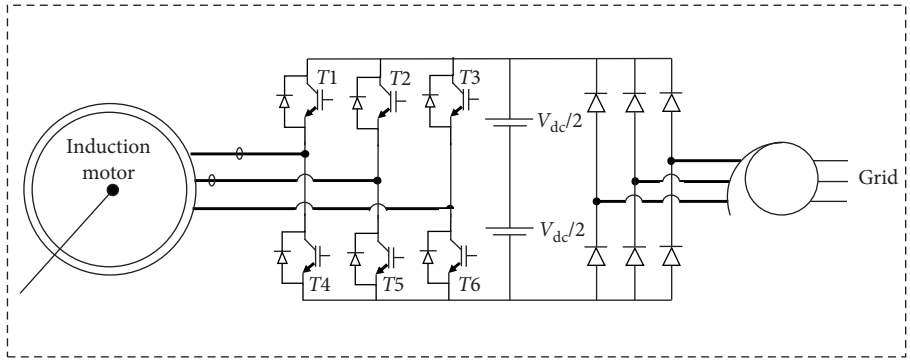

Figure 1: Schematic diagram of the SSTPI-IM drive system (reproduced from M. A. Zdiri et al. 2019 (under the Creative Commons Attribution License/public domain)).

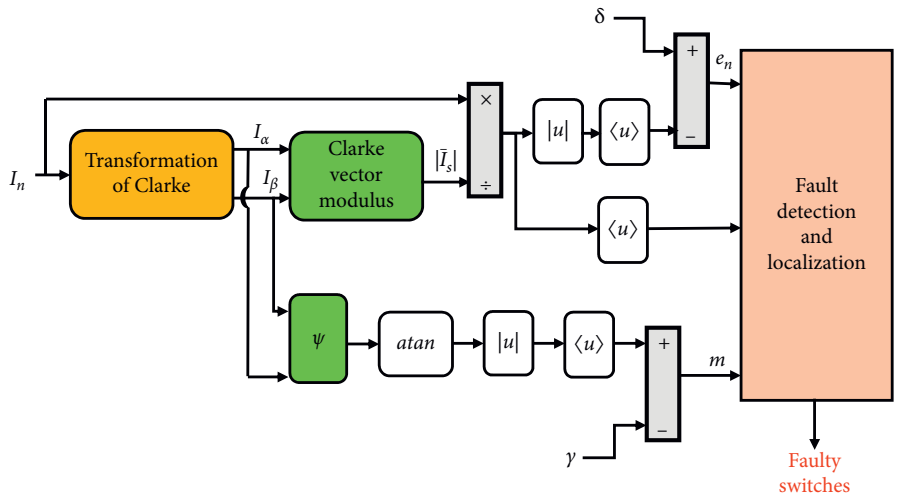

Figure 2: Scheme of the proposed diagnostic method (reproduced from M. A. Zdiri et al. 2019 (under the Creative Commons Attribution License/public domain)).

$$\begin{cases} I_{asN} = \sqrt{\frac{2}{3}}\sin(w_s t) \\ I_{bsN} = \sqrt{\frac{2}{3}}\sin\left(w_s t - \frac{2\pi}{3}\right). \\ I_{csN} = \sqrt{\frac{2}{3}}\sin\left(w_s t + \frac{2\pi}{3}\right) \end{cases} \tag{7}$$

$\langle |I_{nN}| \rangle$, which represent the average absolute values of I_n independently of the maximum amplitude, are presented by

$$\langle |I_{nN}| \rangle = w_s \int_0^{1/w_s} |I_{nN}| \mathrm{d}w_s t. \tag{8}$$

In conclusion, the diagnosis variables ("e_n") are presented by the following equation:

$$e_n = \delta - \langle |I_{nN}| \rangle, \tag{9}$$

where δ represents the average absolute value of I_n in healthy operating conditions, which is equal to 0.5198.

In the OCF case, the diagnosis variables e_n take specific signatures different from those in the healthy case (zero values) depending on the type of fault applied. It can be highlighted that these diagnosis variables only give information about the faulty leg. To completely detect and identify all fault types, the information of the normalized currents average values must be added. To by-pass the drawbacks of the false alarms during speed and load variations, the proposed diagnostic method is also based on the diagnosis variable "m" dedicated from the current slope vector information, which is given by

$$\psi = \frac{I_{\alpha k}}{I_{\beta k}}, \tag{10}$$

where $I_{\alpha k}$ and $I_{\beta k}$ represent the Clarke currents at the time kT_s with T_s denoting the sampling time.

Furthermore, the deviation angle "ϕ" is presented by

$$\phi = \arctan(\psi). \tag{11}$$

Therefore, "$\langle |\phi| \rangle$" is presented by the following equation:

$$\langle|\phi|\rangle = w_s \int_0^{1/w_s} |\phi| \mathrm{d}w_s t. \tag{12}$$

Finally, the diagnosis variable m is obtained from the following equation:

$$m = \langle|\phi|\rangle - \gamma, \tag{13}$$

where γ represents the average absolute value of the deviation angle in the healthy case which is approximately equal to 0.785.

In conclusion, the three diagnosis variables (e_n, s_n, and m) are obtained as follows:

$$E_n = \begin{cases} N & \text{for } e_n < 0 \\ 0 & \text{for } 0 \le e_n < k_f \\ P & \text{for } k_f \le e_n < k_d \\ D & \text{for } e_n \ge k_d \end{cases}, \tag{14}$$

$$S_n = \begin{cases} LL & \text{for } \langle I_{nN}\rangle \le -k_s \\ L & \text{for } -k_s < \langle I_{nN}\rangle < 0 \\ H & \text{for } 0 < \langle I_{nN}\rangle < k_s \\ HH & \text{for } \langle I_{nN}\rangle \ge k_s \end{cases}, \tag{15}$$

$$M = \begin{cases} SS & \text{for } m \le k_p \\ S & \text{for } k_p < m < 0 \\ B & \text{for } 0 < m < k_g \\ BB & \text{for } m \ge k_g \end{cases}. \tag{16}$$

The threshold values (k_f, k_d, k_s, k_p, and k_g) can be analyzed through the study of the diagnosis variable behaviors under healthy and faulty cases [25]. In this work, 27 possible faulty IGBT combinations are addressed in Table 1, where F represents the number of each fault ($F = [1\ 27]$).

In this paper, the diagnosis variables (e_n, s_n, and m) are used only to detect and identify single OCF and phase OCF. Consequently, in order to ameliorate the robustness and to precisely detect and identify these faults without false alarms during speed and load variations, the used diagnosis variables must be processed based on the FLC theory.

3. FLC Theory-Based Diagnostic Method

The FLC theory-based diagnostic method is found on the symptoms of the three diagnosis variables under distinct operating conditions. Indeed, the twelve fault symptoms (N, O, P, D, LL, L, H, HH, SS, S, B, and BB) of the three diagnosis variables ought to be fuzzed using this FLC method. Furthermore, the following section explains this proposed method in more detail.

3.1. Reasoning of the FLC Theory-Based Diagnostic Method. The proposed diagnostic procedure is found on the knowledge of the heuristic and analytical symptoms of the SSTPI behavior under distinct operating conditions. In this paper, the input of the proposed FLC diagnostic method is the symptoms of the diagnosis variables (e_n, s_n, and m). The heuristic knowledge in this proposed diagnostic method is expressed in the form of rules (if then). Moreover, the twelve symptom variables (e_n, s_n, and m) are fuzzified as

$$\begin{cases} E_n \in \{\mathrm{N}, 0, \mathrm{P}, \mathrm{D}\} \\ S_n \in \{\mathrm{LL}, \mathrm{L}, \mathrm{H}, \mathrm{HH}\}. \\ M \in \{\mathrm{SS}, \mathrm{S}, \mathrm{B}, \mathrm{BB}\} \end{cases} \tag{17}$$

The FLC theory bloc is presented in Figure 3, where $F \in [1\ 27]$ as illustrated in Table 1. Indeed, the membership functions of the three diagnosis variables are illustrated in Figure 4.

In the same context, the outputs of the proposed FLC diagnostic method must be also fuzzified based on the membership functions as presented in Figure 5. It is to be highlighted that the fuzzy sets of the inputs and output variables are computed based on trapezoidal and triangular MFs. For example, the output fuzzy set is expressed as follows:

$$\mu_{D-F} = \begin{cases} \dfrac{x-a}{b-a}, & a \le x \le b, \\ 1, & x > b, \end{cases} \tag{18}$$

where a, b, and $x \in [0\ 1]$.

After the fuzzification procedure, the value 0 indicates the healthy case; however, the values between 0 and 1 indicate the faulty case. Accordingly, this proposed fuzzy method can detect and locate the IGBT OCFs without false alarms during speed and load variations which prove their high performance and robustness.

3.2. Extraction of the Fuzzy Rules. Considering the information given in Table 1, the extraction of the fuzzy rules can be determined easily. Generally, the FLC system is composed of fuzzification, fuzzy inference, and defuzzification, as illustrated in Figure 6 [28].

For more details, the fuzzification, fuzzy inference, and defuzzification are explained as follows:

(i) Fuzzification: the fuzzification is based on the MFs, which represents the mapping of the normalized input to the fuzzy variables

(ii) Fuzzy inference: the FLC bloc rules (if then) are characterized by a fuzzy implication linking the input and output fuzzy variables. In this proposed FLC diagnostic method, a fuzzy inference of type Mamdani is used

(iii) Defuzzification: defuzzification denotes the conversion procedure of the fuzzy output to the crisp values. In this paper, the used defuzzification method is the COA method

Accordingly, the fuzzy rules can be well defined as follows:

(i) If $E_{as} = P$ and $E_{bs} = N$ and $E_{cs} = N$ and $S_{as} = L$ and $M = S$, then $D\_1 = \text{Fault}$

Table 1: IGBT OCF detection and identification (reproduced from M. A. Zdiri et al. 2019 (under the Creative Commons Attribution License/public domain)).

F	Faulty IGBTs	E_{as}	E_{bs}	E_{cs}	S_{as}	S_{bs}	S_{cs}	M
1	T1	P	N	N	L			S
2	T4	P	N	N	H			S
3	T2	N	P	N		L		B
4	T5	N	P	N		H		B
5	T3	N	N	P			L	B
6	T6	N	N	P			H	B
7	T1, T4	D						SS
8	T2, T5		D					BB
9	T3, T6			D				BB
10	T1, T2	P	P	N	L	L	H	S
11	T4, T5	P	P	N	H	H	L	S
12	T1, T3	P	N	P	L	H	L	S
13	T4, T6	P	N	P	H	L	H	S
14	T2, T3	N	P	P	H	L	L	BB
15	T5, T6	N	P	P	L	H	H	BB
16	T1, T5				LL	HH		S
17	T2, T4				HH	LL		S
18	T1, T6				LL		HH	S
19	T3, T4				HH		LL	S
20	T2, T6					LL	HH	B
21	T3, T5					HH	LL	B
22	T1, T2, T6	P	P	N	LL	L	HH	S
23	T4, T5, T3	P	P	N	HH	H	LL	S
24	T1, T3, T5	P	N	P	L	HH	LL	S
25	T4, T6, T2	P	N	P	H	LL	HH	S
26	T2, T3, T4	N	P	P	HH	LL	L	B
27	T5, T6, T1	N	P	P	LL	HH	H	B

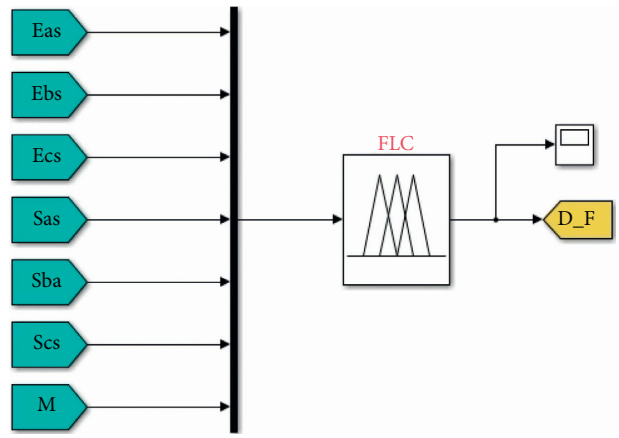

Figure 3: FLC theory bloc.

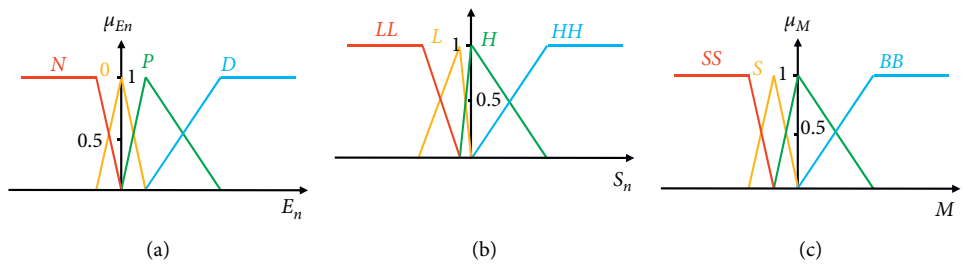

(a) (b) (c)

Figure 4: Membership functions of the proposed FLC theory. (a) μ_{En}, (b) μ_{Sn}, and (c) μ_M.

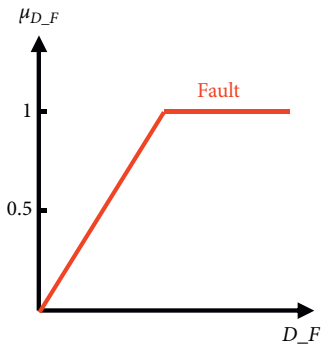

Figure 5: Output membership functions D_F.

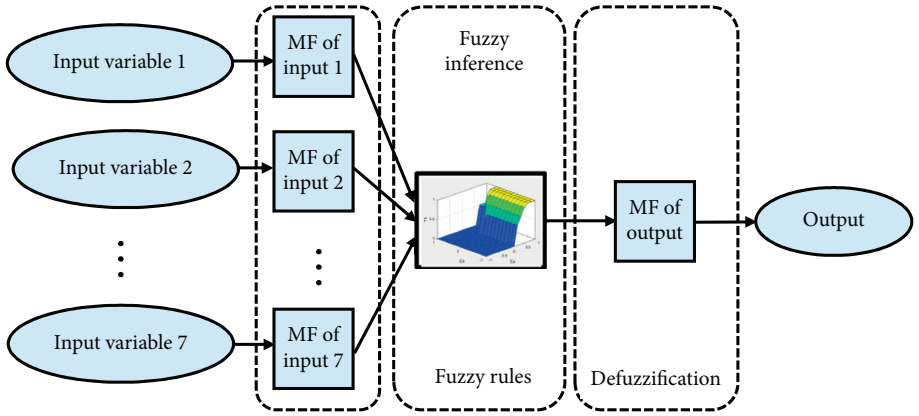

Figure 6: Fuzzy control system bloc.

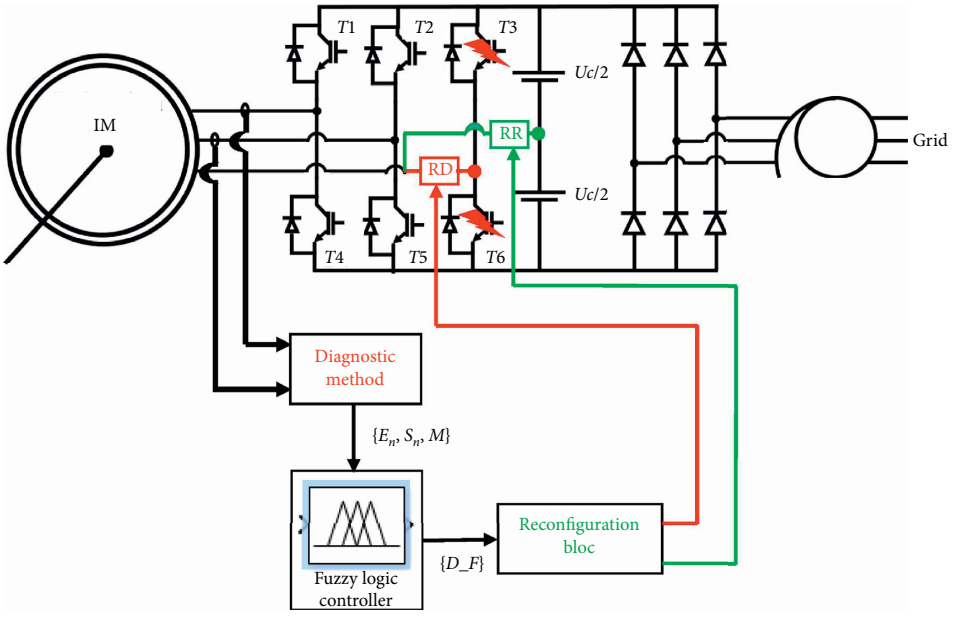

Figure 7: Reconfiguration scheme under third phase OCF.

Table 2: Induction motor parameters. Reproduced from M. A. Zdiri et al. 2019 (under the Creative Commons Attribution License/ public domain).

Rated power (kW)	1.1
Rated line voltage (volt)	600
Supply frequency (Hz)	50
Rated speed (rpm)	2820
Rated load torque (N.m)	3.5
Number of pole pairs	1
Stator resistance (Ω)	6.863
Rotor resistance (Ω)	7.67
Stator inductance (H)	0.708
Rotor inductance (H)	0.708
Mutual inductance (H)	0.684
Moment of inertia (kg.m^2)	0.0033
Friction factor (N.m.s/rad)	0.0035

(ii) If $E_{as} = P$ and $E_{bs} = N$ and $E_{cs} = N$ and $S_{as} = H$ and $M = S$, then $D\_2 = \text{Fault}$

(iii) If $E_{as} = N$ and $E_{bs} = P$ and $E_{cs} = N$ and $S_{bs} = L$ and $M = B$, then $D\_3 = \text{Fault}$

(iv) ⋮

(v) If $E_{as} = N$ and $E_{bs} = P$ and $E_{cs} = P$ and $S_{as} = \text{LL}$ and $S_{bs} = \text{HH}$ and $S_{cs} = H$ and $M = B$, then $D\_27 = \text{Fault}$

Based on these fuzzy rules, the switch faults can be precisely located and detected without false alarms. It is to be underlined that the proposed fuzzy diagnostic method is effective in the reconfiguration step in order to compensate for the fault.

4. Reconfiguration Strategy under IGBT OCFs

In order to compensate the IGBT OCFs after the fault detection using the proposed FLC diagnostic method, we proposed a reconfiguration strategy for the SSTPI-IM association. This strategy is based on using relays without a redundant leg. Furthermore, the implementation of this strategy is easy and low expansive.

In this paper, we focus only on the single and phase OCF. For these faulty cases, the reconfiguration is ensured based on the change of the SSTPI topology to FSTPI topology. Moreover, Figure 7 details well this strategy with respect to an OCF appearance in the third leg of the SSTPI. Referring to Figure 7, the relay "RD" ensures the compensation of the faulty leg; however, the relay "RR" ensures the reconfiguration of the system in order to maintain its continuity. It is worth highlighting that, in the healthy case, the relay RD is ON (activated) while the relay RR is OFF (deactivated).

The reconfiguration bloc is described in further detail as follows:

(i) If $D\_F \neq 0$, then $\text{FR} = 1$

(ii) Else $\text{FR} = 0$

"FR" represents the fault reconfiguration variable. When $\text{FR} = 0$ (healthy case), the relay RD is ON and the relay RR is OFF; however, when $\text{FR} = 1$ (faulty case), the relay RD is OFF and the relay RR is ON in order to compensate for the fault.

5. Simulation Results

To confirm the high performance of the proposed FLC diagnostic method and the reconfiguration strategy, the simulation results are verified through MATLAB/Simulink. Furthermore, the direct RFOC strategy is applied to the SSTPI-IM association with the following IM parameters as illustrated in Table 2. Figure 8 presents the direct RFOC strategy used in this proposed diagnostic method.

For all healthy and faulty cases, the load torque and the reference speed have been taken equal to 1.75 N.m and 200 rad/sec, respectively. Based on the study of all diagnosis variable behaviors under various operating conditions provided in [25], the threshold values k_f, k_d, k_s, k_p, and k_g are equal to 0.06, 0.275, 0.28, -0.408, and 0.161, respectively. After the FLC diagnostic processes, the fault's information can be determined using this proposed diagnostic method.

Concerning the principle of the FLC diagnostic method, Figure 9 illustrates the FLC system of the proposed method. It is to be highlighted that the FLC used in this work is of Mamdani type. For more explanation, Figure 10 presents the fuzzy rule details analyzing the single and phase OCF.

In the healthy case, the IM phase currents are sinusoidal and perfectly balanced as presented in Figure 11. Furthermore, the IM current's information is suitable and can be used by the proposed FLC diagnostic method since there has less harmony distortion rate. Indeed, the FLC process is used also in faulty cases in order to determine the faults information. This information is important in the reconfiguration step in order to compensate for the fault.

5.1. Single Switch OCF. Figure 12 illustrates the simulation results of the three-phase IM currents considering an OCF appearing in the switch T1 at the instant $T = 0.7$ sec.

Indeed, Figure 13 represents the simulation results of the diagnosis variables E_n, normalized current average values S_n, diagnosis variable M, and fuzzy variable $(D - 1)$ considering an OCF appearing in IGBT T1 at $T = 0.7$ sec. Based on Figure 13(a), one can underline that when the T1 OCF occurs, the variable of the faulty phase E_{as} immediately increases; however, the two other diagnosis variables decrease immediately according to Table 1. Furthermore, a decrease of the normalized current average values S_{as} and the diagnosis variable M is obtained. Based on the obtained information of the FLC bloc inputs, the fuzzy variable $D - 1$ differs from zero (the healthy scenario) at the instant $T = 0.7095$ sec.

In conclusion, it can be confirmed that the OCF in IGBT T1 is detected and identified by the proposed FLC diagnostic method at $T = 0.7095$ sec.

5.2. Single Phase OCF. Figure 14 represents the simulation results of the IM currents considering an OCF appearing in the first phase "a" at the instant $T = 0.71$ sec. Furthermore, Figure 15 shows the simulation results of the diagnosis variables E_n, normalized currents average values S_n, diagnosis variable M, and fuzzy variable $D - 7$ considering the same faulty case.

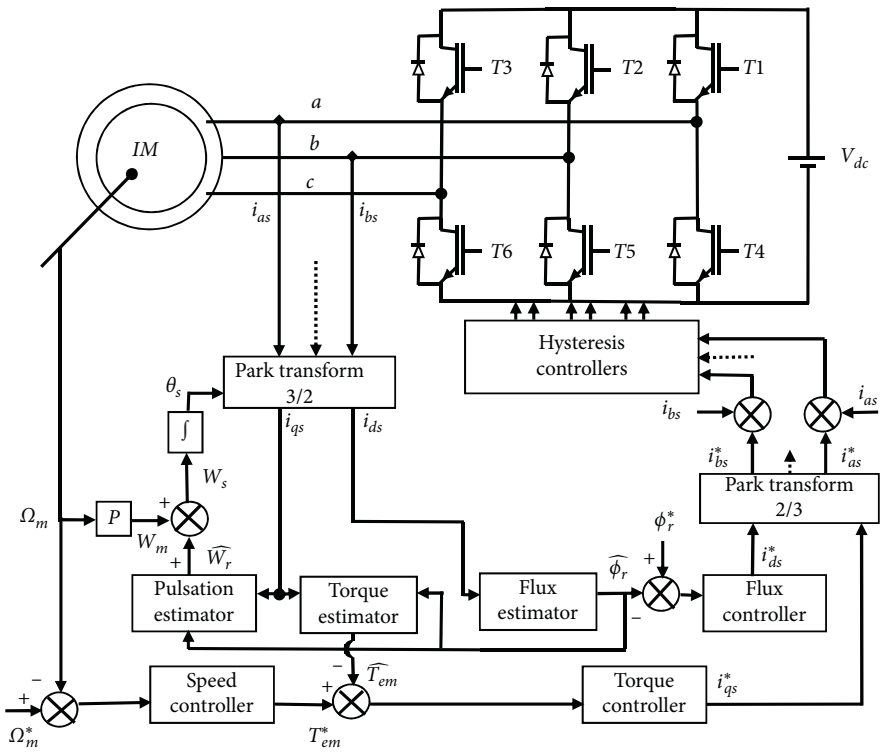

Figure 8: Direct RFOC strategy.

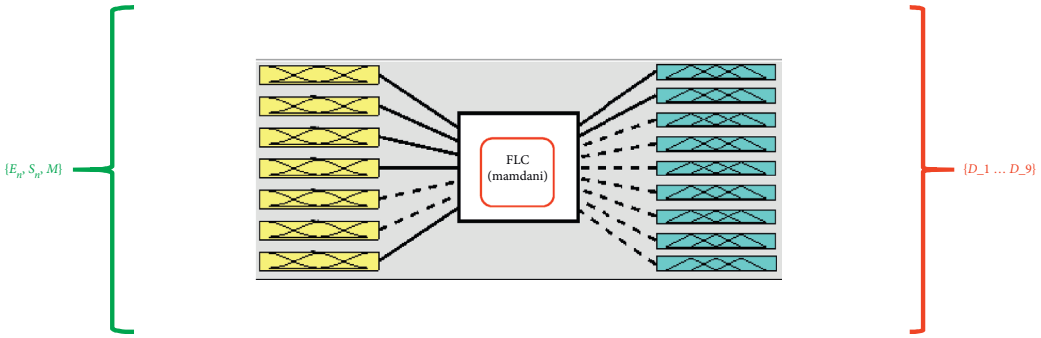

Figure 9: A simulation model of the FLC bloc.

Based on Figure 15, the fuzzy variable $D-7$ is different from zero at the instant $T=0.7168$ sec when the diagnosis variable E_{as} will be high to the threshold value k_d and the diagnosis variable M will be low to the threshold value k_p as presented in Table 1.

In conclusion, one can conclude that the single phase OCF is detected and identified by the proposed FLC diagnostic method at the instant $T=0.7168$ sec. One can confirm that the proposed diagnostic method needs only 0.0068 sec to detect and identify the IGBT OCFs which proves their high performance in terms of rapid fault detection compared to other diagnostic methods.

It should be noted that the suggested FLC diagnostic method is successful in terms of fault reconfiguration when compared to other existing diagnostic methods.

5.3. FLC Diagnostic Method Performance under Load and Speed Variations. This section is aimed to present the robustness of the proposed FLC diagnostic method against the false alarms caused by the variations of the speed and load. To do so, load torque and speed variations versus time have been taken into account as addressed in Figure 16.

Figure 17 shows the simulation results of the IM phase currents under speed and load variations, which are perfectly balanced. Furthermore, Figure 18 shows the simulation results of the diagnosis variables E_n, the variables S_n, the diagnosis variable M, and the fuzzy variable under speed and load variations. Referring to Figure 18, one can confirm that E_n are lower than the obtained thresholds of $\pm$ 0.06, the diagnosis variable M is in the defined range of $[-0.1\ 0.1]$, and the fuzzy variable is equal to zero even with these variations.

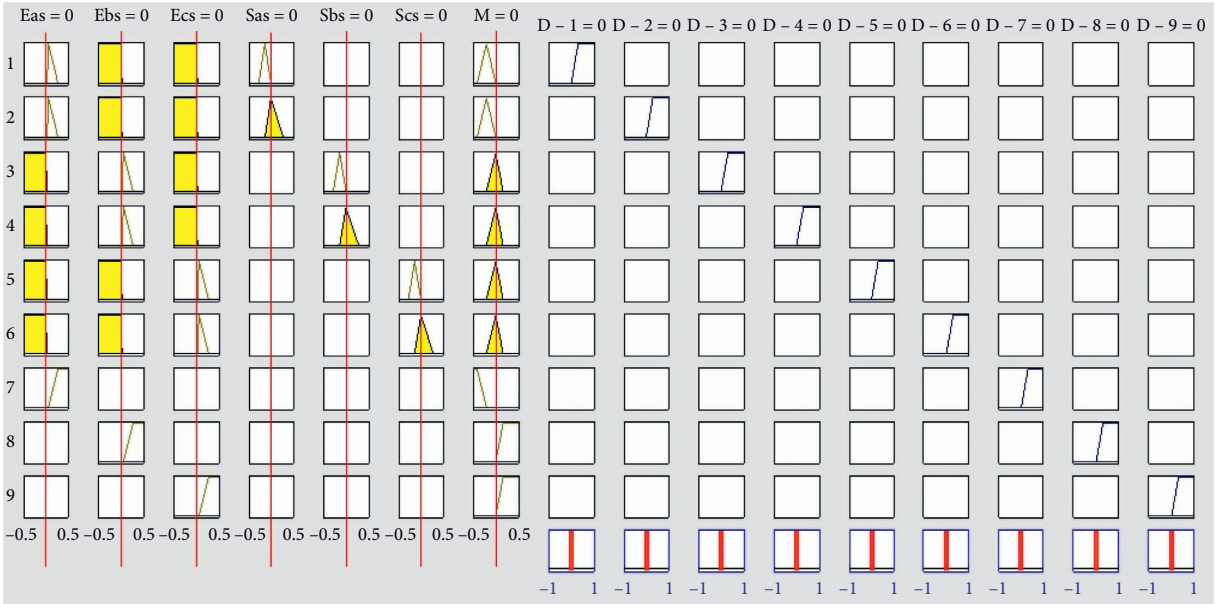

Figure 10: Bloc diagram of the rules of the proposed FLC diagnostic method.

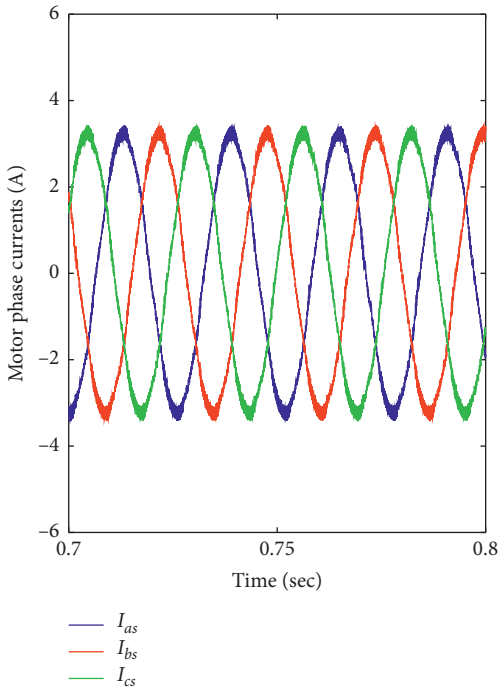

Figure 11: Three-phase IM currents under healthy case.

In conclusion, one can notice the high performance and robustness of the proposed FLC diagnostic method even under speed and load variations in terms of avoiding false alarms. Moreover, the fuzzy variable is equal to zero even under these variations, which makes it easier to obtain the fault reconfiguration information.

5.4. Fault Detection and Reconfiguration. The IM phase currents under an OCF case appearing in IGBT T3 at $T = 0.7$ sec, a reconfiguration case, and a compensation case are presented in Figure 19. Moreover, the simulation results of the SSTPI-fed IM drive considering the healthy, faulty, and compensation cases of the diagnosis variables E_n,

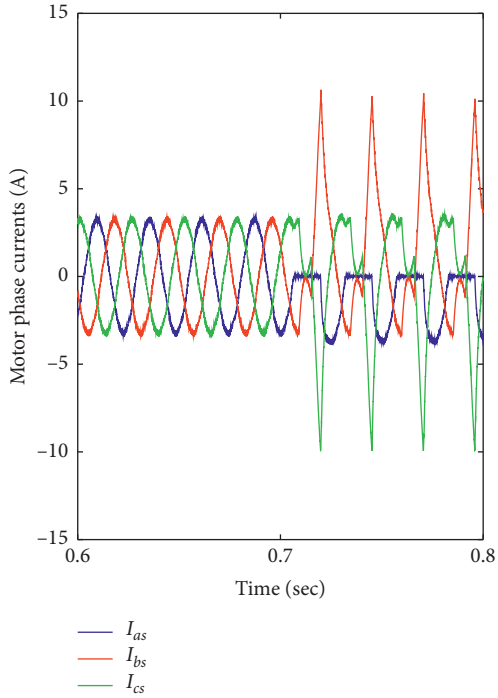

Figure 12: Simulation results of the three-phase IM currents under a single switch OCF in IGBT T1.

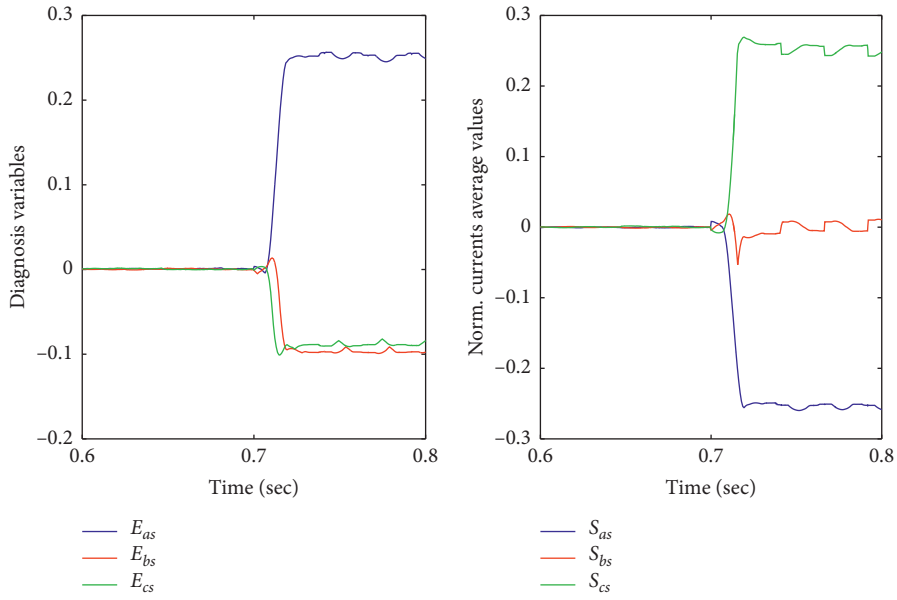

Figure 13: Continued.

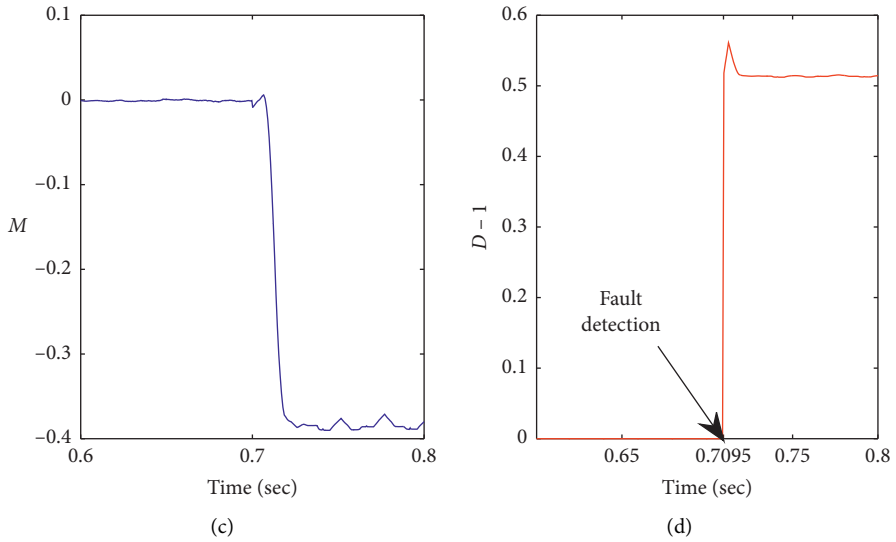

Figure 13: Simulation results of the SSTPI-fed IM drive considering an OCF appearing in T1 at $T = 0.7$ sec. (a) Diagnosis variables E_n, (b) normalized currents average values S_n, (c) diagnosis variable M, and (d) fuzzy variable $(D - 1)$.

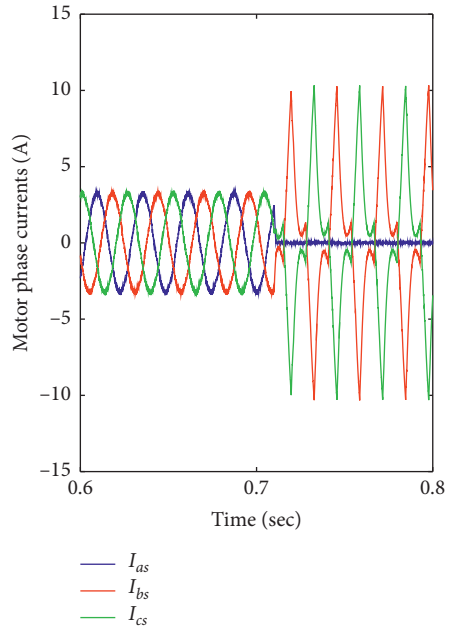

Figure 14: Simulation results of the three-phase IM currents under a single phase OCF in T1 and T4.

normalized currents average values S_n, diagnosis variable M, and FR and fuzzy variable $D - 5$ are illustrated in Figure 20.

Indeed, the T3 IGBT OCF is detected and identified by the proposed FLC diagnostic method when the fuzzy variable $D - 5$ takes a nonzero value, which corresponds to the instant equal to 0.707 sec. Hence, in order to compensate for this fault and maintain the drive system continuity, a step of fault reconfiguration must be applied.

When the fuzzy variable is distinct to the zero value, the reconfiguration variable FR is equal to "1" in order to activate or deactivate the used relays. In this fault case, the reconfiguration strategy is applied by eliminating the faulty leg and ensuring the connection between the fault motor phase and the DC bus middle point. Indeed, the relay RD is deactivated; however, the relay RR is activated in order to maintain the drive system continuity. Furthermore, this

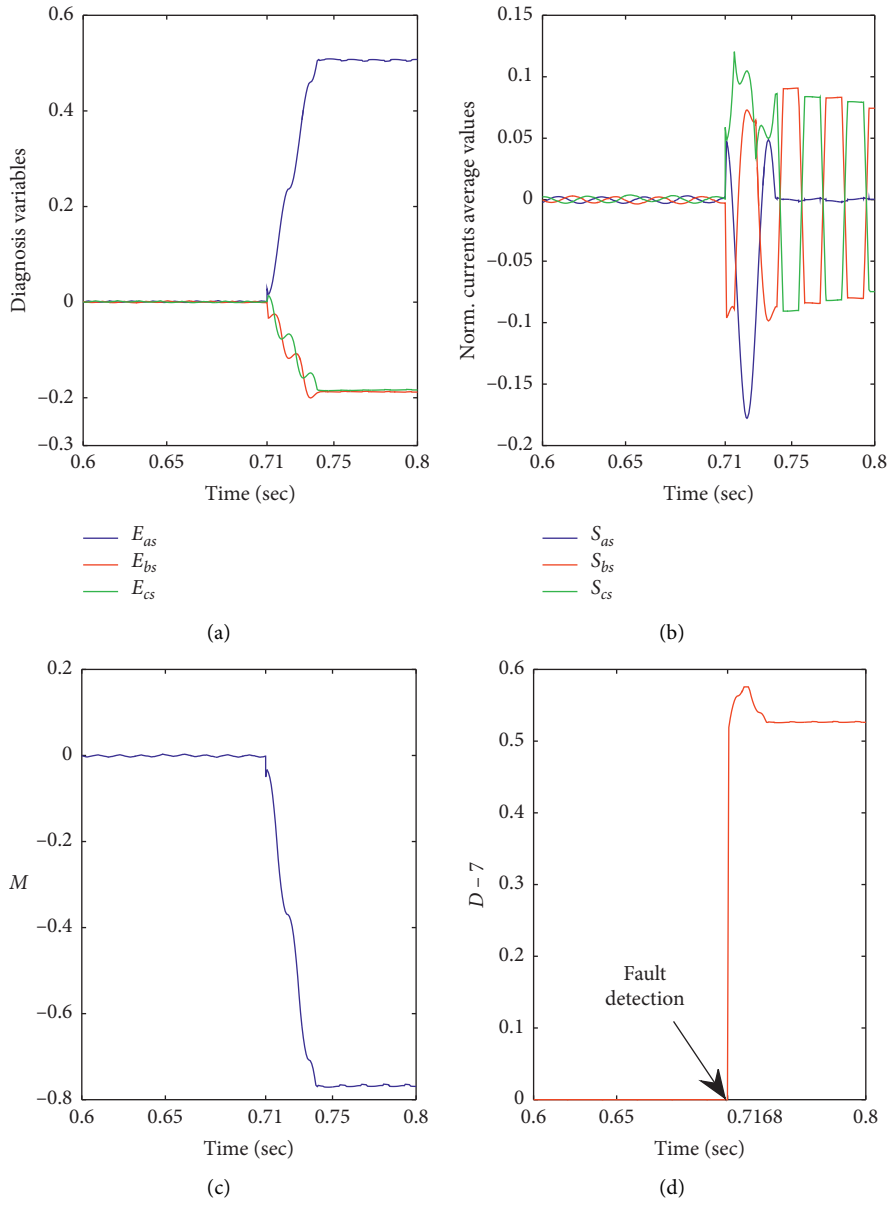

FIGURE 15: Simulation results of the SSTPI-fed IM drive considering an OCF appearing in T1 and T4 at $T = 0.71$ sec. (a) Diagnosis variables E_n, (b) normalized currents average values S_n, (c) diagnosis variable M, and (d) fuzzy variable $(D - 7)$.

reconfiguration step is the same for an OCF appearance in the third phase. After the reconfiguration step, one can confirm that the compensation step is realized when the fuzzy variable returns to zero. It can be underlined that, after the fault compensation, the continuity of the drive system is ensured without power losses.

In conclusion, the proposed FLC diagnostic and reconfiguration methods need only 0.007 sec and 0.33 sec in order to ensure the drive system continuity without power losses, which proves their high performance and effectiveness in terms of fault detection, identification, and compensation.

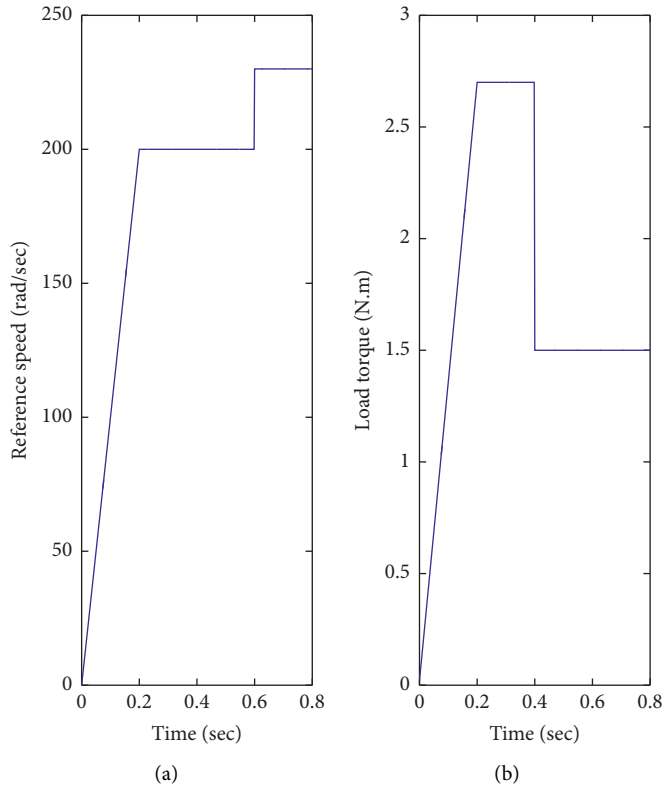

Figure 16: Simulation results of the speed and load variations versus time.

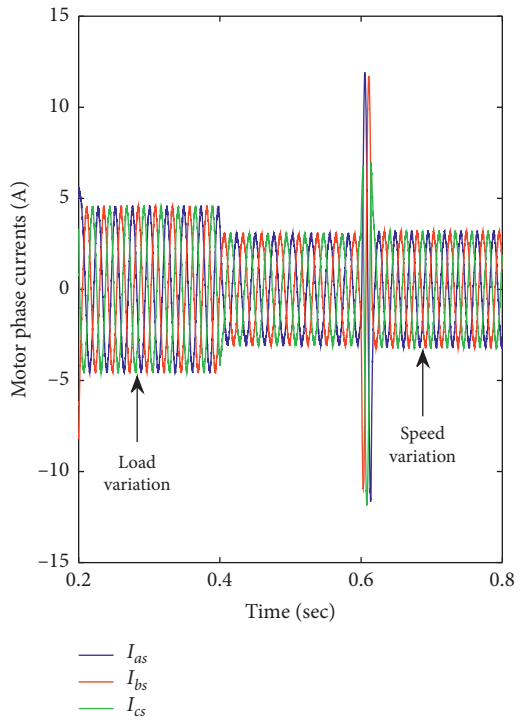

Figure 17: Simulation results of the IM phase currents under speed and load variations.

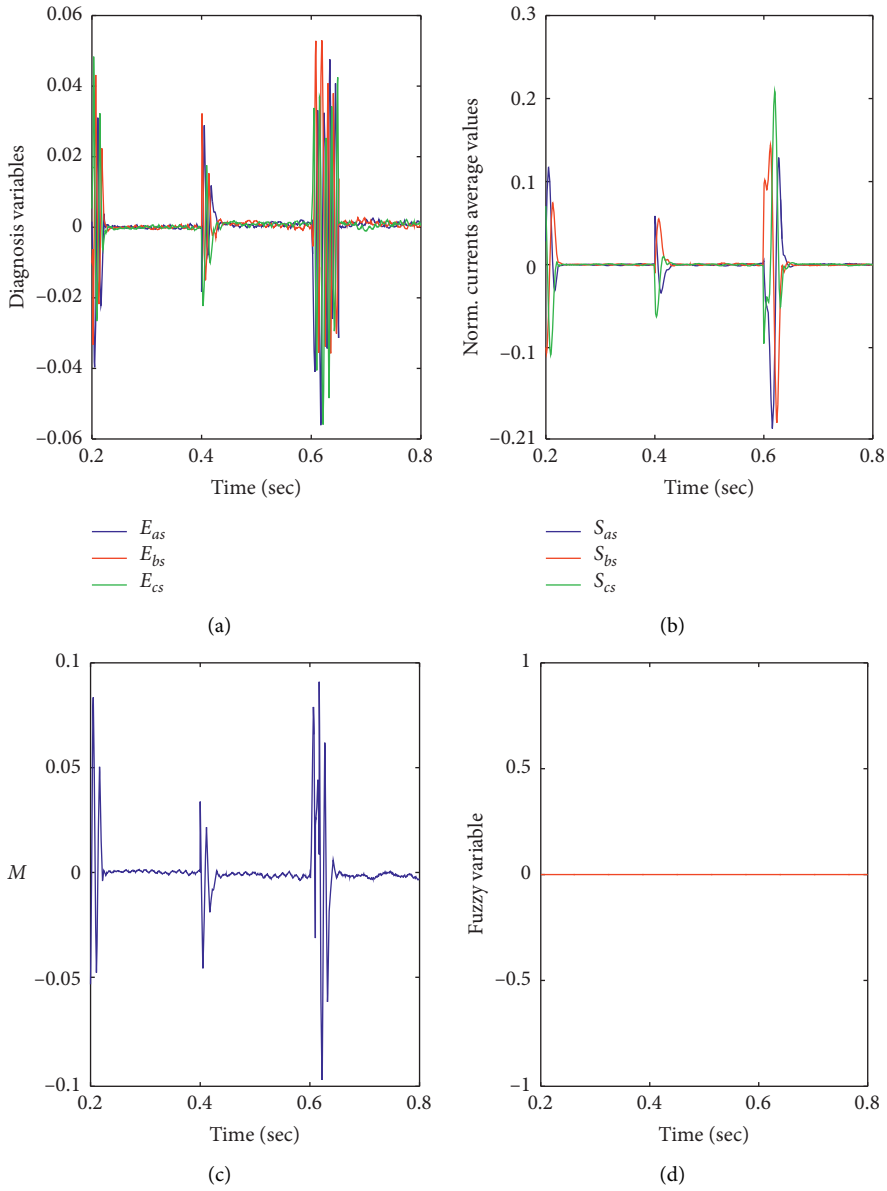

FIGURE 18: Simulation results of the SSTPI-fed IM drive considering load and speed variations. (a) Diagnosis variables E_n, (b) normalized currents average values S_n, (c) diagnosis variable M, and (d) fuzzy variable.

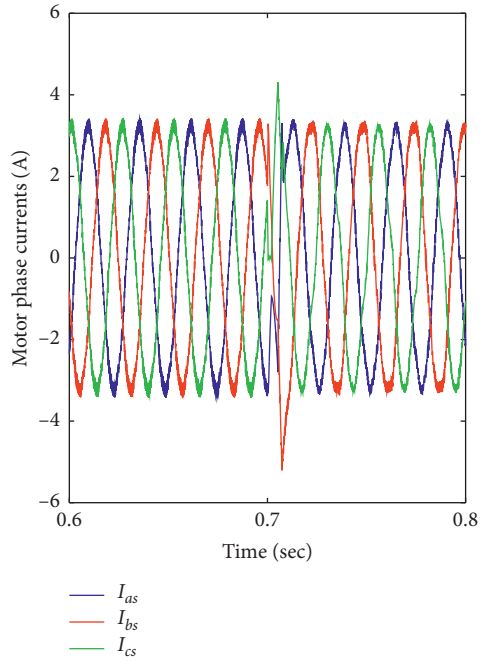

Figure 19: Simulation results of the IM phase currents under the healthy, faulty, and compensation cases.

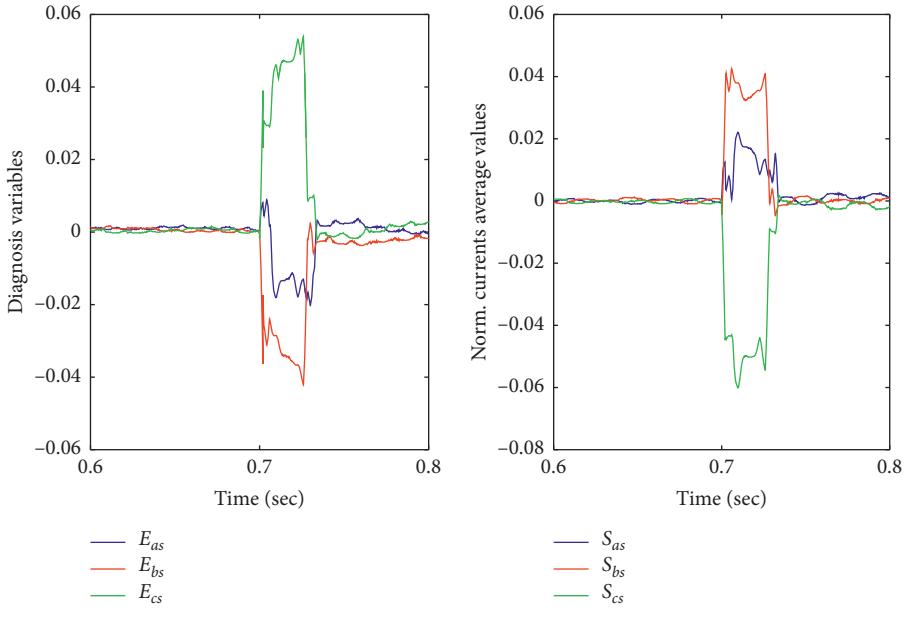

Figure 20: Continued.

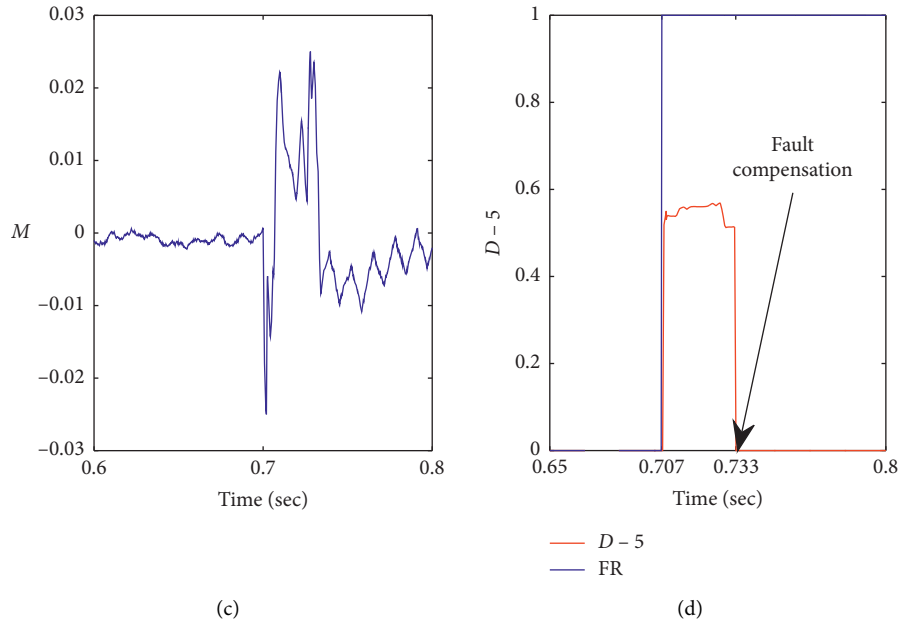

Figure 20: Simulation results of the SSTPI-fed IM drive considering the healthy, faulty, and compensation cases. (a) Diagnosis variables E_n, (b) normalized currents average values S_n, (c) diagnosis variable M, and (d) FR and fuzzy variable $(D-5)$.

6. Conclusion

A novel FLC diagnostic method for the SSTPI-IM drive system has been proposed. This proposed method is based on the measured currents, which avoids the utilization of extra hardware or sensors. In this paper, we focus only on the single OCF and phase OCF appearing in the SSTPI-IM association controlled by the direct RFOC strategy. These faults are detected and identified by using a fuzzy variable, which proves the ability to precisely avoid false alarms during speed and load variations.

After the fault detection and identification based on the fuzzy variable, a fault reconfiguration must be applied to the SSTPI-IM association in order to compensate for the fault and assure the drive system continuity. Indeed, this reconfiguration strategy is found on the change of the SSTPI-IM topology to the FSTPI-IM topology based on using relays without a redundant leg. It can be underlined that, by using this proposed FLC diagnostic and reconfiguration methods, the drive system continues to operate in healthy operating conditions without power losses.

Finally, the simulation results prove to confirm the high performances and effectiveness of the proposed methods in terms of detection, identification, and compensation of the faults without false alarms and power losses. Furthermore, the proposed FLC diagnostic and reconfiguration methods need approximately 0.009 sec and 0.33 sec, respectively, to detect, identify, and compensate the IGBT OCFs. The suggested work can be expanded in light of future directions to other photovoltaic power converters using the combination of fuzzy logic and neural network.

Abbreviations

SSTPI: Six-switch three-phase inverter
FSTPI: Four-switch three-phase inverter
OCFs: Open circuit faults
IGBTs: Insulated gate bipolar transistors
RFOC: Rotor flux oriented control
IM: Induction motor
SCF: Short circuit fault
PWM: Pulse with modulation
VSI: Voltage source inverter
FTC: Fault-tolerant control
FFT: Fast Fourier transform
FDM: Fault detection method
SMO: Sliding mode observer
MMC: Modular multilevel converter
DWT: Discrete wavelet transform
NN: Neural network
MF's: Membership functions
COA: Centroid of area.

Data Availability

No data were used.

Conflicts of Interest

The authors declare that they have no conflicts of interest.

References

[1] L. Jarzebowicz, "Errors of a linear current approximation in high-speed PMSM drives," *IEEE Transactions on Power Electronics*, vol. 32, no. 11, pp. 8254–8257, 2017.

[2] J. Li, M. Sumner, J. A. Padilla, and H. Zhang, "Fault signal propagation through the PMSM motor drive systems," *IEEE Transactions on Industry Applications*, vol. 53, no. 3, pp. 2915–2924, 2017.

[3] J. Ren, Y. Ye, G. Xu, Q. Zhao, and M. Zhu, "Uncertainty-and-Disturbance-Estimator-Based current control scheme for PMSM drives with a simple parameter tuning algorithm," *IEEE Transactions on Power Electronics*, vol. 32, no. 7, pp. 5712–5722, 2017.

[4] B. Lu and S. K. Sharma, "A literature review of IGBT fault diagnostic and protection methods for power inverters," *IEEE Transactions on Industry Applications*, vol. 45, no. 5, pp. 1770–1777, 2009.

[5] A. S. Willsky, "A survey of design methods for failure detection in dynamic systems," *Automatica*, vol. 12, no. 6, pp. 601–611, 1976.

[6] R. Peuget, S. Courtine, and J.-P. Rognon, "Fault detection and isolation on a PWM inverter by knowledge-based model," *IEEE Transactions on Industry Applications*, vol. 34, no. 6, pp. 1318–1326, 1998.

[7] M. Trabelsi, M. Boussak, and M. Gossa, "Multiple IGBTS open circuit faults diagnosis in voltage source inverter fed induction motor using modified slope method," in *Proceedings of The XIX International Conference on Electrical Machines-ICEM 2010*, pp. 1–6, Rome, Italy, September 2010.

[8] S. M. A. Cruz and A. J. M. Cardoso, "Stator winding fault diagnosis in three-phase synchronous and asynchronous motors, by the extended Park's vector approach," *IEEE Transactions on Industry Applications*, vol. 37, no. 5, pp. 1227–1233, 2001.

[9] D. Diallo, M. E. H. Benbouzid, D. Hamad, and X. Pierre, "Fault detection and diagnosis in an induction machine drive: a pattern recognition approach based on concordia stator mean current vector," *IEEE Transactions on Energy Conversion*, vol. 20, no. 3, pp. 512–519, 2005.

[10] J. A. A. Caseiro, A. M. S. Mendes, and A. J. M. Cardoso, "Fault diagnosis on a PWM rectifier ac drive system with fault tolerance using the average current parks vector approach," in *Proceedings of 2009 IEEE International Electric Machines and Drives Conference*, pp. 695–701, Miami, FL, USA, May 2009.

[11] J. O. Estima, N. M. A. Freire, and A. J. M. Cardoso, "Recent advances in fault diagnosis by parks vector approach," in *Proceedings of 2013 IEEE Workshop on Electrical Machines Design, Control and Diagnosis (WEMDCD)*, pp. 279–288, Paris, France, March 2013.

[12] S. Liu, X. Qian, H. Wan, Z. Ye, S. Wu, and X. Ren, "NPC three-level inverter open-circuit fault diagnosis based on adaptive electrical period partition and random forest," *Journal of Sensors*, vol. 2020, Article ID 9206579, 18 pages, 2020.

[13] B. D. E. Cherif and A. Bendiabdellah, "Detection of two-level inverter open-circuit fault using a combined DWT-NN approach," *Journal of Control Science and Engineering*, vol. 2018, Article ID 1976836, 11 pages, 2018.

[14] R. Maamouri, M. Trabelsi, M. Boussak, and F. MSahli, "A sliding mode observer for inverter open-switch fault diagnostic in sensorless induction motor drive," in *Proceedings of IECON 2016-42nd Annual Conference of the IEEE Industrial Electronics Society*, pp. 2153–2158, Florence, Italy, October 2016.

[15] I. Jlassi, J. O. Estima, S. K. El Khil, N. M. Bellaaj, and A. J. M. Cardoso, "A robust observer-based method for IGBTS and current sensors fault diagnosis in voltage-source inverters of PMSM drives," *IEEE Transactions on Industry Applications*, vol. 53, no. 3, pp. 2894–2905, 2017.

[16] S. Shao, P. W. Wheeler, J. C. Clare, and A. J. Watson, "Fault detection for modular multilevel converters based on sliding mode observer," *IEEE Transactions on Power Electronics*, vol. 28, no. 11, pp. 4867–4872, 2013.

[17] C. Gan, J. Wu, S. Yang, Y. Hu, W. Cao, and J. Si, "Fault diagnosis scheme for open-circuit faults in switched reluctance motor drives using fast Fourier transform algorithm with bus current detection," *IET Power Electronics*, vol. 9, no. 1, pp. 20–30, 2016.

[18] L. M. A. Caseiro and A. M. S. Mendes, "Real-time IGBT open-circuit fault diagnosis in three-level neutral-point-clamped voltage-source rectifiers based on instant voltage error," *IEEE Transactions on Industrial Electronics*, vol. 62, no. 3, pp. 1669–1678, 2015.

[19] B. Li, S. Shi, B. Wang, G. Wang, W. Wang, and D. Xu, "Fault diagnosis and tolerant control of single IGBT open-circuit failure in modular multilevel converters," *IEEE Transactions on Power Electronics*, vol. 31, no. 4, pp. 3165–3176, 2016.

[20] M. Syed Ali, N. Gunasekaran, and Q. Zhu, "State estimation of T-S fuzzy delayed neural networks with Markovian jumping parameters using sampled-data control," *Fuzzy Sets and Systems*, vol. 306, pp. 87–104, 2017.

[21] N. Gunasekaran, R. Saravanakumar, Y. H. Joo, and H. S. Kim, "Finite-time synchronization of sampled-data T-S fuzzy complex dynamical networks subject to average dwell-time approach," *Fuzzy Sets and Systems*, vol. 374, pp. 40–59, 2019.

[22] E. Yucel, M. Syed Ali, N. Gunasekaran, and S. Arik, "Sampled-data filtering of Takagi-Sugeno fuzzy neural networks with interval time-varying delays," *Fuzzy Sets and Systems*, vol. 316, pp. 69–81, 2017.

[23] K. Das, S. Samanta, U. Naseem, S. Khalid Khan, and K. De, "Application of fuzzy logic in the ranking of academic institutions," *Fuzzy Information and Engineering*, vol. 11, no. 3, pp. 295–306, 2019.

[24] K. Das, S. Samanta, K. De, X. Encarnacion, and C. B. Das, "Ranking of educational institutions using fuzzy logic: a mathematical approach," *Afrika Matematika*, vol. 31, no. 7-8, pp. 1295–1310, 2020.

[25] M. A. Zdiri, B. Bouzidi, and H. Hadj Abdallah, "Performance investigation of an advanced diagnostic method for SSTPI-fed IM drives under single and multiple open IGBT faults," *COMPEL-The International Journal for Computation and Mathematics in Electrical and Electronic Engineering*, vol. 38, no. 2, pp. 616–641, 2019.

[26] M. A. Zdiri, B. Bouzidi, M. B. Ammar, and H. H. Abdallah, "SSTPI-IM reconfiguration and diagnostic under OCF appearance used in PV system," *International Journal of Renewable Energy Research (IJRER)*, vol. 11, no. 1, pp. 20–30, 2021.

[27] M. A. Zdiri, M. Ben Ammar, B. Bouzidi, R. Abdelhamid, and H. H. Abdallah, "An advanced switch failure diagnosis method and fault tolerant strategy in photovoltaic boost

converter," *Electric Power Components and Systems*, vol. 48, no. 18, pp. 1932–1944, 2020.

[28] Z. Liu, Z. Zheng, and Y. Li, "Enhancing fault-tolerant ability of a nine-phase induction motor drive system using fuzzy logic current controllers," *IEEE Transactions on Energy Conversion*, vol. 32, no. 2, pp. 759–769, 2017.